HHS Public Access

Author manuscript

Mech Dev. Author manuscript; available in PMC 2019 June 01.

Published in final edited form as:

Mech Dev. 2018 June ; 151: 10–17. doi:10.1016/j.mod.2018.04.001.

Ift25 Is Not a Cystic Kidney Disease Gene but Is Required for Early Steps of Kidney Development

Paurav B. Desai[1], **Jovenal T. San Agustin**[1], **Michael W. Stuck**[1], **Julie A. Jonassen**[2], **Carlton M. Bates**[3], and **Gregory J. Pazour**[1,‡]

[1]Program in Molecular Medicine, University of Massachusetts Medical School, Biotech II, Suite 213, 373 Plantation Street, Worcester, MA 01605

[2]Department of Microbiology and Physiological Systems, University of Massachusetts Medical School, 55 Lake Avenue North, Worcester MA 01655

[3]Department of Pediatrics, University of Pittsburgh, Children's Hospital of Pittsburgh of UPMC, 5130 Rangos Research Center, 4401 Penn Avenue, Pittsburgh, PA 15224

Abstract

Eukaryotic cilia are assembled by intraflagellar transport (IFT) where large protein complexes called IFT particles move ciliary components from the cell body to the cilium. Defects in most IFT particle proteins disrupt ciliary assembly and cause mid gestational lethality in the mouse. IFT25 and IFT27 are unusual components of IFT-B in that they are not required for ciliary assembly and mutant mice survive to term. The mutants die shortly after birth with numerous organ defects including duplex kidneys. Completely duplex kidneys result from defects in ureteric bud formation at the earliest steps of metanephric kidney development. Ureteric bud initiation is a highly regulated process involving reciprocal signaling between the ureteric epithelium and the overlying metanephric mesenchyme with regulation by the peri-Wolffian duct stroma. The finding of duplex kidney in *Ift25* and *Ift27* mutants suggests functions for these genes in regulation of ureteric bud initiation. Typically the deletion of IFT genes in the kidney causes rapid cyst growth in the early postnatal period. In contrast, the loss of *Ift25* results in smaller kidneys, which show only mild tubule dilations that become apparent in adulthood. The smaller kidneys appear to result from reduced branching in the developing metanephric kidney. This work indicates that IFT25 and IFT27 are important players in the early development of the kidney and suggest that duplex kidney is part of the ciliopathy spectrum.

Keywords

intraflagellar transport; Hedgehog signaling; cilia; duplex kidney; kidney development

‡Corresponding Author: Telephone: 508 856 8078, gregory.pazour@umassmed.edu.

Introduction

During mammalian development, cilia play critical roles in breaking left-right symmetry and in organizing the hedgehog signaling pathway. Ciliary dysfunction causes a wide variety of disorders collectively known as the ciliopathies that include birth defects affecting most organs. In the kidney, cilia are well known for their roles in maintaining tubule architecture and preventing cyst formation. Recently, we noted that mutations in a number of cilia-related genes caused duplex kidney formation (San Agustin et al., 2016). This malformation, which is known in humans as duplicated collecting duct system, is thought to be caused by the formation of extraneous ureteric buds at the first steps in development of the metanephric kidney. Duplex ureteric buds can interact separately with the metanephric mesenchyme leading to a duplex kidney with upper and lower poles drained separately by individual ureters. Often one of the ureters does not connect to the bladder properly or even at all, leading to obstruction, reflux of urine from the bladder to the kidney, and/or risks of infection.

Germline loss of *Ift25* and *Ift27* caused duplex kidney with high frequency (Keady et al., 2012; Eguether et al., 2014). These proteins are subunits of the intraflagellar transport (IFT) complex B. The IFT system is required for ciliary assembly and is thought to be responsible for transporting the 1000 or more ciliary proteins from their sites of synthesis in the cell body to the organelle in order to build and maintain the structure. Unlike most other complex B proteins, these two subunits are not needed for ciliary assembly but are needed for hedgehog signaling. Activation of the hedgehog pathway begins with sonic hedgehog or another hedgehog ligand binding to its receptor patched-1. This causes patched-1 to exit the cilium, allows smoothened to activate and accumulate in the cilium. Smoothened then activates the downstream steps of the pathway to reduce the production of the Gli3R, promote the activation of Gli2 and the expression of Gli1 to drive expression of a few hundred genes under control of the hedgehog pathway.

Kidney development in the mouse begins with the formation of the pronephros at about 8 days of gestation. In mammals, the pronephros is not thought to be functional in regulating body fluid composition, but is needed for the development of the second or mesonephric kidney. The mesonephric kidney consists of a small number of glomeruli connected to the Wolffian duct and drains into the cloaca. While the mesonephric kidney may play some role in regulating body fluid composition, it importantly provides the platform for development of the third or metanephric kidney, which is the functional kidney in the mature animal. Development of the metanephric kidney in mouse begins on about E10.5 with the outgrowth a bud from the base of the Wolffian duct near the point of insertion into the cloaca. The growth of the bud is regulated by complex signaling between the ureteric epithelium of the Wolffian duct and the overlying metanephric mesenchyme and peri-Wolffian duct stroma. Bud formation on the Wolffian duct is stimulated by metanephric mesenchyme-derived GDNF. If unchecked, GDNF would stimulate supernumerary buds, but GDNF activity is antagonized by Slit2/Robo2 signaling and BMP4 secretion from peri-Wolffian duct stroma (Miyazaki et al., 2000; Grieshammer et al., 2004). A small region of BMP4 activity is in turn antagonized by Gremlin to allow a single bud to form. Lack of GDNF causes kidney agenesis, the lack of BMP4 results in extraneous bud formation and the loss of Gremlin

causes kidney agenesis. The ureteric bud grows out from the Wolffian ducts and branches to become the collecting duct system of the kidney and the main stalk becomes the ureter. Signals from the ureteric epithelium induce the metanephric mesenchyme to become the nephrons (Costantini and Shakya, 2006; Little and McMahon, 2012; Desgrange and Cereghini, 2015).

In this work we examine the role of the IFT proteins IFT25 and IFT27 in kidney development and the cystic kidney disease. Germline deletion of either gene causes duplex kidneys with high frequency. Interestingly, specific deletion of *Ift25* in either collecting duct or metanephric mesenchyme is not sufficient to produce duplex kidneys but deletion in the peri-Wolffian duct stroma is sufficient. Unlike other IFT genes, collecting duct deletion of *Ift25* does not cause cystic kidney disease but instead results in smaller kidneys that develop only mild tubule dilation with age.

Experimental Procedures

Mouse Breeding

The *Ift25* and *Ift27* mutant mice were generated with ES cells from the KOMP and EUCOMM projects. The initial mice carried the neo (Tm1a) alleles, which contained a genetrap insertion and selectable marker, but had all exons intact. The null alleles (Tm1b) were generated by deleting the floxed exon from the germ line with Prm-Cre (O'Gorman et al., 1997) and the flox alleles (Tm1c) were generated by deleting the genetrap insertion and selectable marker from the germline with FlpE (Farley et al., 2000). See supplemental data in (Keady et al., 2012; Eguether et al., 2014) for diagrams. The flox alleles were deleted in kidney lineages using HoxB7-Cre (Yu et al., 2002), Rarb2-Cre (Kobayashi et al., 2005) and Tbx18-Cre (Wang et al., 2009). Tamoxifen-inducible CAGG-Cre^{ER} (Hayashi and McMahon, 2002) was used to delete at specific time points in development. Pregnant mice were given 0.1 ml of 10 mg/ml tamoxifen (in canola oil) by oral gavage. Cre activity was monitored by use of the mTmG reporter line (Muzumdar et al., 2007). All lines except the Tbx18-Cre were C57Bl/6J congenics maintained by recurrent mating to wild type C57Bl/6J purchased from Jackson Laboratory. Tbx18-Cre animals were a mix of C57Bl/6J and FVB/N.

Mouse work was carried out at the University of Massachusetts Medical School and the University of Pittsburgh with IACUC approval.

Histology

Hematoxylin and Eosin—Paraffin sections for H&E staining were dewaxed with Safeclear (Fisher Scientific, Hampton, NH) and rehydrated with graded aqueous solutions of isopropanol. The sections were stained for 4 min with CAT Hematoxylin (Biocare Medical, Concord, CA), rinsed in running tap water for 30 sec followed by three quick dips in saturated lithium carbonate and a rinse in distilled water. This was followed by 90% ethanol for 2 min, Edgar Degas Eosin (Biocare Medical) for 2 min and 3 quick rinses in 100% ethanol. The sections were cleared with Safeclear (two 5 min incubations) and were mounted with Permount (Fisher Scientific).

Immunofluorescence—Paraffin sections were dewaxed, rehydrated and subjected to antigen retrieval in an autoclave (250°F, 40 min) with 10 mM sodium citrate at pH 6. Sections were brought to ambient temperature and treated with blocking solution (4% non-immune goat serum, 0.1% Triton X-100, 0.05% SDS, and 0.1% fish skin gelatin [Sigma] in TBST [0.05% Tween-20 in Tris-buffered saline, pH 7.4]) for 30 minutes, subsequently washed with TBST and then exposed to primary antibodies overnight at 4°C. Next day the sections were washed with TBST, incubated with Alexa Fluor-conjugated secondary antibodies (Life Technologies, Grand Island, NY) for 30 min at 22°C, and washed with TBST followed by a rinse with TBS. The antibodies were brought to their working dilutions with 0.1% fish skin gelatin in TBS. The sections were then dipped for 5 seconds in DAPI (1 μg/ml in TBS) and after rinsing with TBS were mounted with Prolong Gold (Life Technologies). Confocal images were acquired with an inverted microscope (TE-2000E2; Nikon) equipped with a Solamere Technology – modified spinning disk confocal scan head (CSU10; Yokogawa). Z stacks were acquired at 0.5- micron intervals and converted to single planes by maximum projection with MetaMorph software (MDS Analytical Technologies).

Antibodies used included Arl13b (Neuromab, University of California Davis, clone N295B/66), gamma tubulin (Sigma, clone GTU88) and aquaporin-2 (Sigma, rabbit polyclonal).

Branching Morphogenesis—E13.5 mice were collected and fixed with 4% paraformaldehyde (in PBS, pH 7.4) overnight on ice and in the dark. Embryos were washed with PBS three times for 15 minutes each. After embedding in 2% low melt agarose, 150 micron sections were serially cut with a Microslicer DTK-1000 vibratome (Ted Pella Incorporated). The sections were stained with Dolichos Biflorus Agglutinin (1:100 dilution, Vector Laboratories) overnight, washed with PBS and imaged with a Zeiss Discovery V12 Stereo microscope equipped with a Zeiss AxioCam MRc camera. Terminal end buds were counted blind to the genotype.

Results

Ift25 and *Ift27* mutants have pleiotropic structural birth defects including duplex kidneys

IFT25 and IFT27 form a stable heterodimer within IFT complex B (Bhogaraju et al., 2011). However, the mouse phenotypes are unusual as *Ift25* and *Ift27* mutants survive to term and are born alive whereas most other IFT-B mutants die at mid gestation. The *Ift25* and *Ift27* mutants die shortly after birth and have structural defects in most organs including the kidneys, where duplicated collecting duct system and/or duplex kidney is often observed. Five out of twelve *Ift25* mutants examined showed at least one duplex kidney while 12 out of 25 *Ift27* mutants examined had this phenotype [Figure 1 and (Keady et al., 2012; Eguether et al., 2014)].

Motile cilia defects do not cause duplex kidneys

During a large-scale ENU screen (Li et al., 2015), we noted that many cilia-defective lines exhibited duplex kidneys (San Agustin et al., 2016). This included many lines with mutations only expected to affect motile cilia. Possible reasons for this result are that the findings reflect the prevalence of duplex kidney in the C57Bl/6J inbred mouse strain or that

motile cilia are involved in regulating ureteric bud formation on the Wolffian duct. The placement of kidneys differs on the right and left sides of mammals. The right mouse kidney is located more cranially than the left, while humans show the opposite placement with the left located more cranially than the right. One possibility for this arrangement is that the positon of the ureteric bud is controlled by the left-right pattern, which is established by motile cilia in the embryonic node. To test involvement of the node in formation of duplex kidneys, we used the tamoxifen-inducible CAGG-Cre^{ER} to delete *Ift25* at various time points in development. Since the node acts to break left-right symmetry about E7.5 and the ureteric buds form at about E10.5 we deleted at E6.5, E7.5 and E8.5 and collected kidneys for serial-section H&E analysis on E13.5 and E14.5 (Figure 2A). Deletion on E6.5 resulted in one experimental animal with bilateral duplex kidneys and three with normal kidneys (not shown). Deletion on E7.5 resulted in one experimental animal with a unilateral duplex kidney and one with normal kidneys (not shown). Deletion on E8.5 resulted in three experimental animals with unilateral duplex kidneys and two with normal kidneys (Figure 2B). It is unclear how fast the *Ift25* gene is deleted and the gene product decays. However, finding duplex kidneys in animals treated on E8.5 clearly shows that the role of IFT25 in ureteric bud formation occurs after the left-right pattern is established.

As discussed above, we identified many examples of duplex kidneys in lines with mutations in ciliary motility genes during our large scale ENU mouse screen suggested that motile cilia may contribute to the duplex kidney phenotype (Li et al., 2015). However, it was difficult to estimate penetrance of kidney phenotypes in the large-scale screen as structural heart defects were the primary focus of the screen and kidney phenotypes were not fully characterized in all animals. To more carefully determine the penetrance of duplex kidney in a line with a motile cilia defect, we collected kidneys from twelve mutant animals from the *Dnah5*^{b2b002Clo} line, which was a line that presented duplex kidneys in the ENU screen. *Dnah5* encodes a subunit of outer arm dynein and is expected to affect motile cilia but not non-motile primary cilia. Serial section H&E staining of these 12 pairs of kidneys did not detect any examples of duplex kidney (Supplemental Figure 1). This finding indicates that the incidence of duplex kidney in the *Dnah5* mutant line is quite rare and does not support a role for motile cilia in duplex kidney formation.

Conditional deletion of IFT25 from the peri-Wolffian duct stroma results in duplex kidneys

The formation of a single ureteric bud on the Wolffian duct is thought to be the result of complex reciprocal signaling between the ureteric epithelium and renal mesenchyme with regulation by signals from the peri-Wolffian duct stroma. Germline deletions of *Ift25* or *Ift27*, which showed duplex kidneys with a penetrance of ~50%, lack the gene products in all lineages. To understand their importance in each lineage, we used HoxB7-Cre, Rarb2-Cre and Tbx18-Cre to specifically delete *Ift25* in the ureteric epithelium, the renal mesenchyme and the peri-Wolffian duct stroma respectively. Serial section H&E analysis of 12 experimental animals where *Ift25* was deleted by HoxB7-Cre and 15 experimental animals where *Ift25* was deleted by Rarb2-Cre showed no instances of duplex kidney while deletion with Tbx18-Cre resulted in one animal showing duplex kidney out of eleven examined (Figure 3). The mTmG Cre activity reporter showed that the Rarb2-Cre and HoxB7-Cre recombinases were active in the expected cell types (data not shown). This suggests that the

peri-Wolffian duct stroma is an important site of IFT25 action in regulating the reciprocal signaling between the ureteric epithelium and the renal mesenchyme. However the lower penetrance seen in the tissue specific deletions as compared to the germline deletion may suggest that gene function has to be lost in more than one tissue to produce the phenotype.

IFT25 is not a cystic kidney disease gene

The loss of many *Ift* genes from the kidney results in cyst formation leading to end stage renal disease (Pazour et al., 2000; Davenport et al., 2007; Jonassen et al., 2008; Jonassen et al., 2012; Tran et al., 2014). To learn if IFT25 also contributes to cystic disease, we collected kidneys from animals where *Ift25* was deleted from the ureteric epithelium by HoxB7-Cre. Deletion of *Ift20* or *Ift140* by this Cre results in rapid cyst formation in the early postnatal period with end stage renal disease occurring by three to four weeks of age (Jonassen et al., 2008; Jonassen et al., 2012). At P20, we observed no evidence of cyst formation by H&E staining (not shown) and curiously the kidney to body weight ratio was slightly reduced (1.60%±0.097 in controls, 1.51%±0.061 in experimentals, p=0.025 by unpaired t test) (Figure 4A). At this point, *Ift20* or *Ift140*-deleted kidneys would have ratios of ~15% (Jonassen et al., 2008; Jonassen et al., 2012). Since these animals were healthy, we followed them out to P80. Like at P20, the kidneys at P80 were not cystic although mild dilations of some tubules were observed (Figure 4B). Also, similar to what we observed at P20, the kidney to body weight ratio were smaller in the *Ift25*-deleted animals (1.37%±0.11 in controls, 1.25%±0.072 in experimentals, p=0.012 by unpaired t test) (Figure 4A). The ratio appears to be driven by the mutants having smaller kidneys rather than having larger bodies (Supplemental Figure 2A, B). In cultured fibroblasts, we did not observe any defects in percent ciliation or cilia length when *Ift25* or *Ift27* were defective. At both P20 and P80, there was slight reduction in the percent of collecting duct cells that were ciliated (Figure 4D) although the cilia that remained were normal length (Supplemental Figure 2C).

A reduced amount of ureteric branching could cause the smaller sized kidneys observed when *Ift25* was deleted. To test this, we serially sectioned kidneys collected from E13.5 embryos whose ureteric epithelium was labeled with GFP and counted the end buds. Examination of three control animals and three *Ift25* mutants showed a slight but significant reduction in the number of buds (82.0±7.6 in controls and 62.7±6.5 in *Ift25* mutants, p=0.028 by unpaired t test).

Discussion

In this work, we examined the role of the atypical IFT-B proteins IFT25 and IFT27 in kidney development and cystic kidney disease. Germline mutations in eithergen e result in duplex kidney formation. This structural birth defect is thought to result when the ureteric epithelium of the Wolffian duct does not receive proper signals from themetanephric mesenchyme and peri-Wolffian duct stroma at the earliest steps of formation of the metanephric or permanent kidney. In mammalian development, cilia play important roles in breaking of left-right symmetry and regulation of hedgehog signaling. The finding of duplex kidneys in a large number of ciliary genes initially suggested that duplex kidney could be caused by disturbances of left-right patterning but tamoxifen-induced deletions ruled out this

possibility. Thus it is likely that cilia are acting through hedgehog signaling to control ureteric bud formation although it is possible that a currently unknown cilia-regulated pathway may contribute. Hedgehog is known to control gene expression patterns critical for early kidney development (Gill and Rosenblum, 2006) and genetic studies have implicated hedgehog signaling in many aspects of early kidney development. Attenuation of hedgehog signaling by germline deletion of the gene encoding sonic hedgehog results in renal aplasia and dysplasia(Hu et al., 2006) while t he loss of this gene from the ureteric epithelium resultsin hypoplastic kidneys with hydronephrosis and hydroureter (Yu et al., 2002). The germline loss of Smo results in embryonic lethality prior to metanephric kidney development. Smo deletion from the ureteric epithelium does not cause detectable phenotypes (Cain et al., 2009) although expression of constitutively active Smo in the ureteric epithelium leads to renal hypoplasia and hydronephrosis (Gupta et al., 2017).

Hedgehog signaling converges on three transcription factors, Gli1, Gli2 and Gli3. Interestingly, certain Gli3 alleles cause duplex kidney similar to what is seen in *Ift25* and *Ift27* mutants (Blake et al., 2016). In the absence of hedgehog ligand, Gli3 is normally processed to a smaller Gli3R form that acts as a transcriptional repressor. Upon pathway activation Gli3R is degraded relieving its inhibitory activity. Gli3 mutations in humans result in Pallister-Hall syndrome and Greig cephalopolysyndactyly. Greig cephalopolysyndactyly is marked by polydactyly, syndactyly, craniofacial abnormalities and macrocephaly and while Pallister-Hall syndrome patients show polydactyly, syndactyly, hypothalamic hamartomas, imperforate anus and kidney anomalies including aplasia and hypoplasia. It is thought that Greig cephalopolysyndactyly is caused by missense mutations resulting in haploinsufficiency of the Gli3 protein. Pallister-Hall syndrome is caused by a variety of mutations that all result in gene products similar to Gli3R suggesting that it is due to unregulated production of a repressor form of Gli3 (Hall, 2014). Duplex kidneys are observed in mice carrying the $Gli3^{\Delta 699}$ allele (Blake et al., 2016). This allele was originally thought to be a Gli3R mimic. However later analysis showed that the Gli3R phenotype is distinct from $Gli3^{\Delta 699}$ and suggests that $Gli3^{\Delta 699}$ is more likely to be a hypomorphic allele (Cao et al., 2013).

Ift25 and *Ift27* mutations reduce the amount of Gli3R that is made in the limb bud and also in cultured fibroblasts (Keady et al., 2012; Eguether et al., 2014). In the limb bud, Gli3R antagonizes gremlin to reduce its activity (Litingtung et al., 2002; Zuniga, 2015). In the kidney, gremlin is an important regulator of ureteric bud formation that acts by antagonizing BMP4 to allow the pro-budding signal GDNF to stimulate the formation of a single ureteric bud from the Wolffian duct. If Gli3R antagonizes gremlin in the developing kidney as it does in the limb bud, a straightforward model of how IFT25 and IFT27 cause duplex kidneys can be formulated (Figure 6). In this model, the loss of IFT25 or IFT27 reduces Gli3R. The lower Gli3R activity allows expanded gremlin activity and since gremlin is an antagonist of BMP4, then GDNF activity would be increased leading to extraneous ureteric buds. This model is consistent with our observation that duplex kidney resulted when *Ift25* was deleted in the peri-Wolffian duct stroma as this is the site of BMP4 activity that regulates ureteric bud formation from the Wolffian duct (Miyazaki et al., 2000).

The lack of cyst formation when *Ift25* was deleted by HoxB7-Cre was unexpected as every other example of *Ift* gene disruption in kidney resulted in cystic disease (Pazour et al., 2000; Davenport et al., 2007; Jonassen et al., 2008; Jonassen et al., 2012; Tran et al., 2014). The lack of cysts probably reflects the fact that cilia are still formed in *Ift25* mutants as compared to other *Ift* mutants. The precise role of cilia in maintaining tubule architecture and preventing cyst formation is not known but proposals include flow sensing (Nauli et al., 2003), regulation of Wnt signaling (Merkel et al., 2007) and perhaps even hedgehog signaling (Tran et al., 2014). As discussed above, hedgehog signaling plays important roles in kidney development but the role in cyst formation is not as well established. However recent work suggests that attenuating hedgehog signaling reduces cyst growth (Tran et al., 2014). This would be consistent with our finding of reduced hedgehog signaling in *Ift25* mutants and the lack of cyst formation in these animals. However, the role of cilia is likely very complicated as loss of cilia is sufficient to drive cyst formation but the loss of cilia from polycystin-2 mutants reduces cyst growth (Ma et al., 2013) indicating that cilia have both pro-cystic and anti-cystic functions.

Supplementary Material

Refer to Web version on PubMed Central for supplementary material.

Acknowledgments

We thank Dr. P. Odgren for use of his bright field microscope, Dr. A. Walker for use of her dissecting microscope, Dr. J. Richter for use of his vibratome, Dr. C. Lo for collecting the Dnah5 material and Abigail Smith for assistance with imaging. This work was supported by the National Institutes of Health GM060992 and DK103632 to GJP and DK095748 to CMB. Core resources supported by the Diabetes Endocrinology Research Center grant DK32520 and the Alabama Recessive Polycystic Kidney Disease Core Center DK074038 were used.

Abbreviations

IFT	intraflagellar transport
H&E	hematoxylin and eosin

References

Bhogaraju S, Taschner M, Morawetz M, Basquin C, Lorentzen E. Crystal structure of the intraflagellar transport complex 25/27. EMBO J. 2011; 30:1907–1918. [PubMed: 21505417]

Blake J, Hu D, Cain JE, Rosenblum ND. Urogenital development in Pallister-Hall syndrome is disrupted in a cell-lineage-specific manner by constitutive expression of GLI3 repressor. Hum Mol Genet. 2016; 25:437–447. [PubMed: 26604140]

Cain JE, Islam E, Haxho F, Chen L, Bridgewater D, Nieuwenhuis E, Hui CC, Rosenblum ND. GLI3 repressor controls nephron number via regulation of Wnt11 and Ret in ureteric tip cells. PLoS One. 2009; 4:e7313. [PubMed: 19809516]

Cao T, Wang C, Yang M, Wu C, Wang B. Mouse limbs expressing only the Gli3 repressor resemble those of Sonic hedgehog mutants. Dev Biol. 2013; 379:221–228. [PubMed: 23644062]

Costantini F, Shakya R. GDNF/Ret signaling and the development of the kidney. BioEssays. 2006; 28:117–127. [PubMed: 16435290]

Davenport JR, Watts AJ, Roper VC, Croyle MJ, van Groen T, Wyss JM, Nagy TR, Kesterson RA, Yoder BK. Disruption of intraflagellar transport in adult mice leads to obesity and slow-onset cystic kidney disease. Curr Biol. 2007; 17:1586–1594. [PubMed: 17825558]

Desgrange A, Cereghini S. Nephron Patterning: Lessons from Xenopus, Zebrafish, and Mouse Studies. Cells. 2015; 4:483–499. [PubMed: 26378582]

Eguether T, San Agustin JT, Keady BT, Jonassen JA, Liang Y, Francis R, Tobita K, Johnson CA, Abdelhamed ZA, Lo CW, Pazour GJ. IFT27 Links the BBSome to IFT for Maintenance of the Ciliary Signaling Compartment. Dev Cell. 2014; 31:279–290. [PubMed: 25446516]

Farley FW, Soriano P, Steffen LS, Dymecki SM. Widespread recombinase expression using FLPeR (flipper) mice. Genesis. 2000; 28:106–110. [PubMed: 11105051]

Gill PS, Rosenblum ND. Control of murine kidney development by sonic hedgehog and its GLI effectors. Cell Cycle. 2006; 5:1426–1430. [PubMed: 16855389]

Grieshammer U, Le M, Plump AS, Wang F, Tessier-Lavigne M, Martin GR. SLIT2-mediated ROBO2 signaling restricts kidney induction to a single site. Dev Cell. 2004; 6:709–717. [PubMed: 15130495]

Gupta DP, Hwang JW, Cho ES, Kim W, Song CH, Chai OH. Constitutive Activation of Smoothened in the Renal Collecting Ducts Leads to Renal Hypoplasia, Hydronephrosis, and Hydroureter. Cells Tissues Organs. 2017; 204:38–48. [PubMed: 28564646]

Hall JG. Pallister-Hall syndrome has gone the way of modern medical genetics. Am J Med Genet C Semin Med Genet. 2014; 166C:414–418. [PubMed: 25424727]

Hayashi S, McMahon AP. Efficient recombination in diverse tissues by a tamoxifen-inducible form of Cre: a tool for temporally regulated gene activation/inactivation in the mouse. Dev Biol. 2002; 244:305–318. [PubMed: 11944939]

Hu MC, Mo R, Bhella S, Wilson CW, Chuang PT, Hui CC, Rosenblum ND. GLI3-dependent transcriptional repression of Gli1, Gli2 and kidney patterning genes disrupts renal morphogenesis. Development. 2006; 133:569–578. [PubMed: 16396903]

Jonassen JA, San Agustin J, Follit JA, Pazour GJ. Deletion of IFT20 in the mouse kidney causes misorientation of the mitotic spindle and cystic kidney disease. J Cell Biol. 2008; 183:377–384. [PubMed: 18981227]

Jonassen JA, SanAgustin J, Baker SP, Pazour GJ. Disruption of IFT complex A causes cystic kidneys without mitotic spindle misorientation. J Am Soc Nephrol. 2012; 23:641–651. [PubMed: 22282595]

Keady BT, Samtani R, Tobita K, Tsuchya M, San Agustin JT, Follit JA, Jonassen JA, Subramanian R, Lo CW, Pazour GJ. IFT25 links the signal-dependent movement of Hedgehog components to intraflagellar transport. Dev Cell. 2012; 22:940–951. [PubMed: 22595669]

Kobayashi A, Kwan KM, Carroll TJ, McMahon AP, Mendelsohn CL, Behringer RR. Distinct and sequential tissue-specific activities of the LIM-class homeobox gene Lim1 for tubular morphogenesis during kidney development. Development. 2005; 132:2809–2823. [PubMed: 15930111]

Li Y, Klena NT, Gabriel GC, Liu X, Kim AJ, Lemke K, Chen Y, Chatterjee B, Devine W, Damerla RR, Chang C, Yagi H, San Agustin JT, Thahir M, Anderton S, Lawhead C, Vescovi A, Pratt H, Morgan J, Haynes L, Smith CL, Eppig JT, Reinholdt L, Francis R, Leatherbury L, Ganapathiraju MK, Tobita K, Pazour GJ, Lo CW. Global genetic analysis in mice unveils central role for cilia in congenital heart disease. Nature. 2015

Litingtung Y, Dahn RD, Li Y, Fallon JF, Chiang C. Shh and Gli3 are dispensable for limb skeleton formation but regulate digit number and identity. Nature. 2002; 418:979–983. [PubMed: 12198547]

Little MH, McMahon AP. Mammalian kidney development: principles, progress, and projections. Cold Spring Harb Perspect Biol. 2012:4.

Ma M, Tian X, Igarashi P, Pazour GJ, Somlo S. Loss of cilia suppresses cyst growth in genetic models of autosomal dominant polycystic kidney disease. Nat Genet. 2013; 45:1004–1012. [PubMed: 23892607]

Merkel CE, Karner CM, Carroll TJ. Molecular regulation of kidney development: is the answer blowing in the Wnt? Pediatr Nephrol. 2007; 22:1825–1838. [PubMed: 17554566]

Miyazaki Y, Oshima K, Fogo A, Hogan BL, Ichikawa I. Bone morphogenetic protein 4 regulates the budding site and elongation of the mouse ureter. J Clin Invest. 2000; 105:863–873. [PubMed: 10749566]

Muzumdar MD, Tasic B, Miyamichi K, Li L, Luo L. A global double-fluorescent Cre reporter mouse. Genesis. 2007; 45:593–605. [PubMed: 17868096]

Nauli SM, Alenghat FJ, Luo Y, Williams E, Vassilev P, Li X, Elia AE, Lu W, Brown EM, Quinn SJ, Ingber DE, Zhou J. Polycystins 1 and 2 mediate mechanosensation in the primary cilium of kidney cells. Nat Genet. 2003; 33:129–137. [PubMed: 12514735]

O'Gorman S, Dagenais NA, Qian M, Marchuk Y. Protomine-Cre recombinase transgene efficiently recombine target sequences in the male germ line of mice, but not in embryonic stem cells. Proc Nat Acad Sci USA. 1997; 94:14602–14607. [PubMed: 9405659]

Pazour GJ, Dickert BL, Vucica Y, Seeley ES, Rosenbaum JL, Witman GB, Cole DG. *Chlamydomonas IFT*88 and its mouse homologue, polycystic kidney disease gene *Tg737*, are required for assembly of cilia and flagella. J Cell Biol. 2000; 151:709–718. [PubMed: 11062270]

San Agustin JT, Klena N, Granath K, Panigrahy A, Stewart E, Devine W, Strittmatter L, Jonassen JA, Liu X, Lo CW, Pazour GJ. Genetic link between renal birth defects and congenital heart disease. Nat Commun. 2016; 7:11103. [PubMed: 27002738]

Tran PV, Talbott GC, Turbe-Doan A, Jacobs DT, Schonfeld MP, Silva LM, Chatterjee A, Prysak M, Allard BA, Beier DR. Downregulating hedgehog signaling reduces renal cystogenic potential of mouse models. J Am Soc Nephrol. 2014; 25:2201–2212. [PubMed: 24700869]

Wang Y, Tripathi P, Guo Q, Coussens M, Ma L, Chen F. Cre/lox recombination in the lower urinary tract. Genesis. 2009; 47:409–413. [PubMed: 19415630]

Yu J, Carroll TJ, McMahon AP. Sonic hedgehog regulates proliferation and differentiation of mesenchymal cells in the mouse metanephric kidney. Development. 2002; 129:5301–5312. [PubMed: 12399320]

Zuniga A. Next generation limb development and evolution: old questions, new perspectives. Development. 2015; 142:3810–3820. [PubMed: 26577204]

Highlights

- Mutations in *Ift25* and *Ift27* cause duplex kidney
- Unlike other *Ift* genes, loss of *Ift25* from kidney collecting ducts does not cause cyst formation
- Loss of *Ift25* from kidney collecting ducts results in smaller kidneys with reduced branching

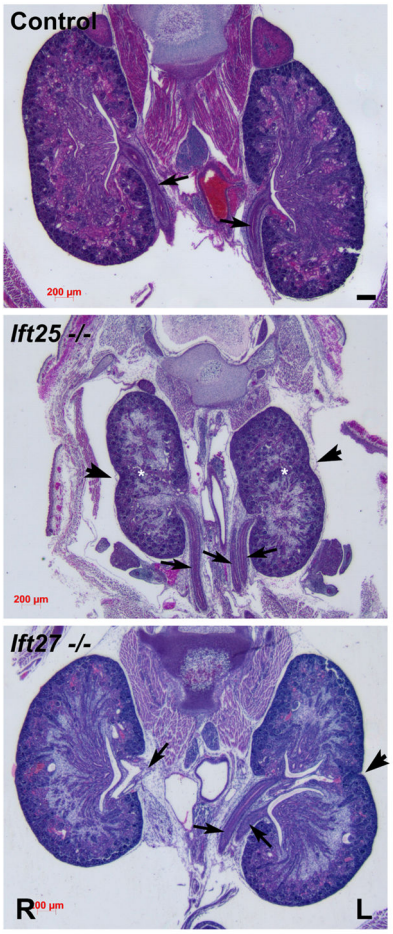

Figure 1. *Ift25* and *Ift27* null mutants form duplex kidneys

H&E stained sections of E18 control, *Ift25* and *Ift27* mutant kidneys. Note that this *Ift25* mutant is bilaterally duplex while this *Ift27* mutant is unilaterally duplex on the left side. Duplex kidneys can be identified by two ureters attached to a single kidney (arrows) or by a constriction in the kidney capsule (arrow heads) often accompanied by a cortical septum or hypertrophied Column of Bertin extending towards the medulla (*). Five of 12 *Ift25* mutants (Keady et al., 2012) and 12 of 25 *Ift27* mutants (Eguether et al., 2014) had at least one duplex kidney. Scale bar is 200 microns and applies to all images in figure. L, left; R, right.

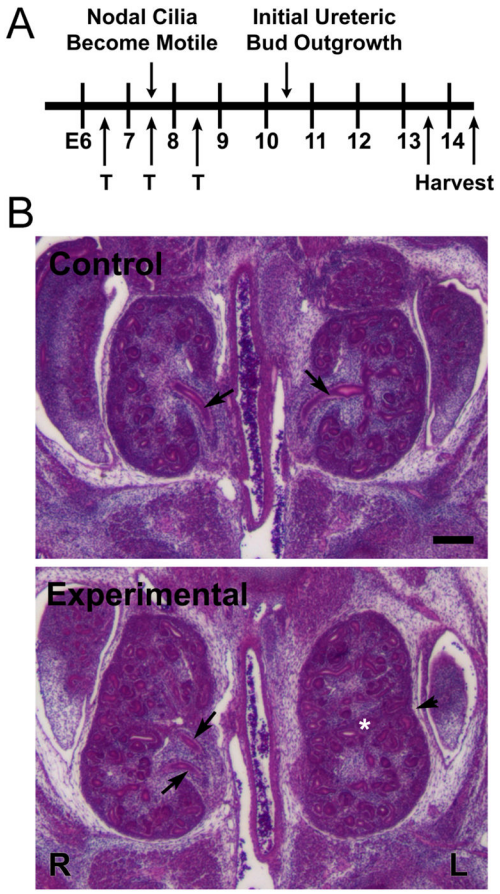

Figure 2. Deletion of *Ift25* after node formation results in duplex kidneys

A. Timeline of the experiment. Timed pregnant mice were treated with tamoxifen (T) (1 mg by oral gavage) at embryonic day 6.5, 7.5 or 8.5 and harvested at either E13.5 or E14.5. The time of initiation of nodal cilia motility (E7.5) and the initiation of ureteric bud outgrowth from the Wolffian duct toward the metanephric mesenchyme (E10.5) are marked above the line.

B. Control and experimental animals treated on E8.5 and harvested on E14.5. Note the control animal has a single ureter (arrows) on both sides. The experimental animal is bilaterally duplex. The right kidney has two ureters (arrows) while the left kidney shows the constriction (arrow head) and cortical septum (asterisk) consistent with duplex kidneys. Scale bar is 200 microns and applies to both images. L, left; R, right.

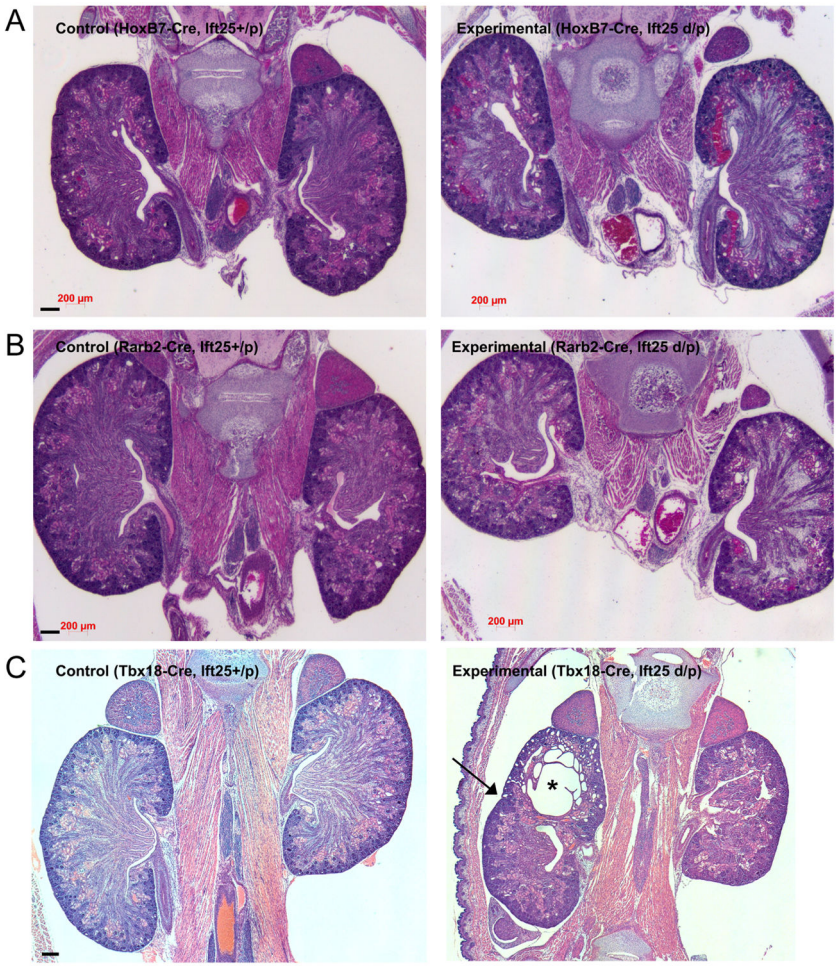

Figure 3. Conditional deletion of *Ift25* in the peri-Wolffian duct stroma results in duplex kidneys

A. H&E stained sections of E18 kidneys with *Ift25* deleted in the ureteric lineage with the HoxB7-Cre. No duplex kidneys were observed in 12 experimental kidneys that were serially sectioned. Scale bar is 200 microns. d, null allele; p, floxed allele.

B. H&E stained sections of E18 kidneys with *Ift25* deleted in the metanephric mesenchymal lineages with the Rarb2-Cre. No duplex kidneys were observed in 15 experimental kidneys that were serially sectioned. Scale bar is 200 microns. d, deletion allele; p, floxed allele.

C. H&E stained sections of E18 kidneys with *Ift25* deleted in the peri-Wolffian duct stroma with the Tbx18-Cre. One duplex kidney was observed in 11 experimental kidneys that were serially sectioned. Scale bar is 200 microns. d, null allele; p, floxed allele.

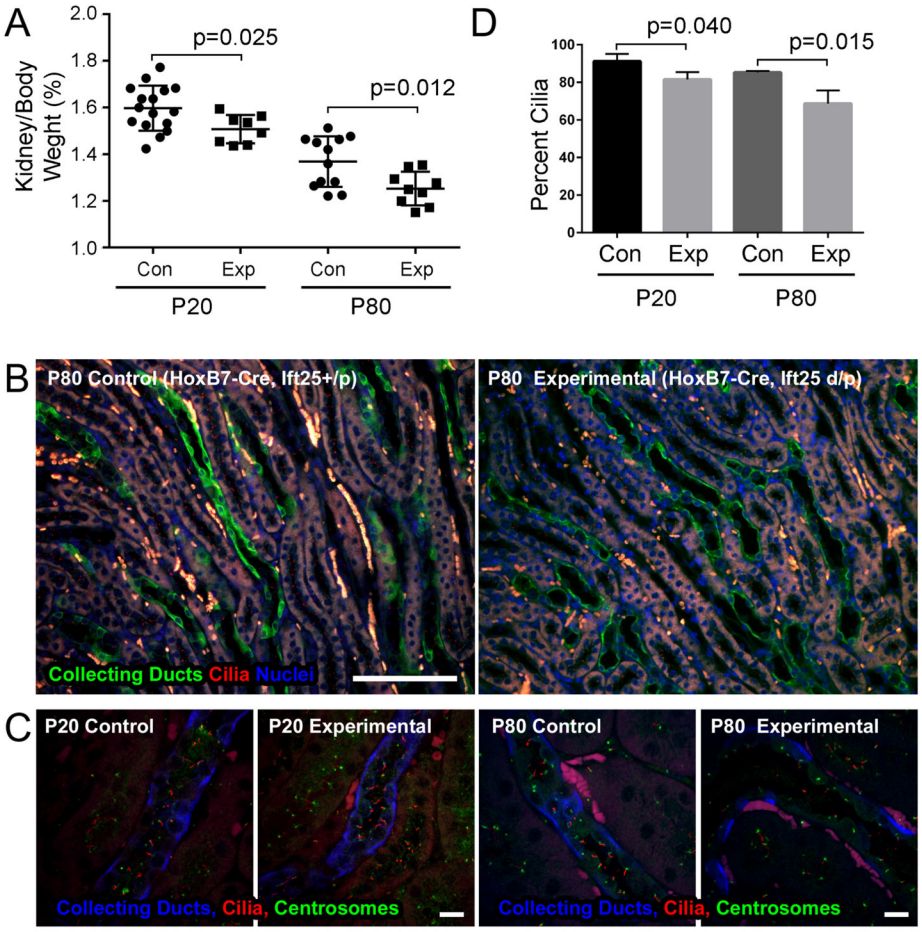

Figure 4. Deletion of *Ift25* by *HoxB7-Cre* Reduces Kidney to Body Weight Ratio

A. Kidney to body weight ratio is reduced when *Ift25* is deleted by *HoxB7-Cre*. Each point represents an individual animal. P values were determined by unpaired t test.

B. Collecting ducts (Aquaporin-2, green; DAPI, blue) are slightly dilated in P80 animals when *Ift25* is deleted by *HoxB7-Cre*. Cilia (Arl13b, red) are present in both genotypes. Each image is a maximum projection of 16 confocal images taken at 0.5 micron intervals. Scale bar is 100 microns. d, null allele; p, floxed allele.

C.D. Cilia (Arl13b, red) per centrosome (or centrosome pair in G2 cells) (gamma tubulin, green) are slightly reduced in collecting ducts (Aquaporin-2, blue) at both P20 and P80 when *Ift25* is deleted by *HoxB7-Cre*. No difference was observed in length of non-zero length cilia (see Supplemental Figure 2C). N=3 animals for each and >100 centrosomes counted per animal. Each image is a maximum projection of 16 confocal images taken at 0.5 micron intervals. Scale bars are 10 microns. P values were determined by unpaired t test.

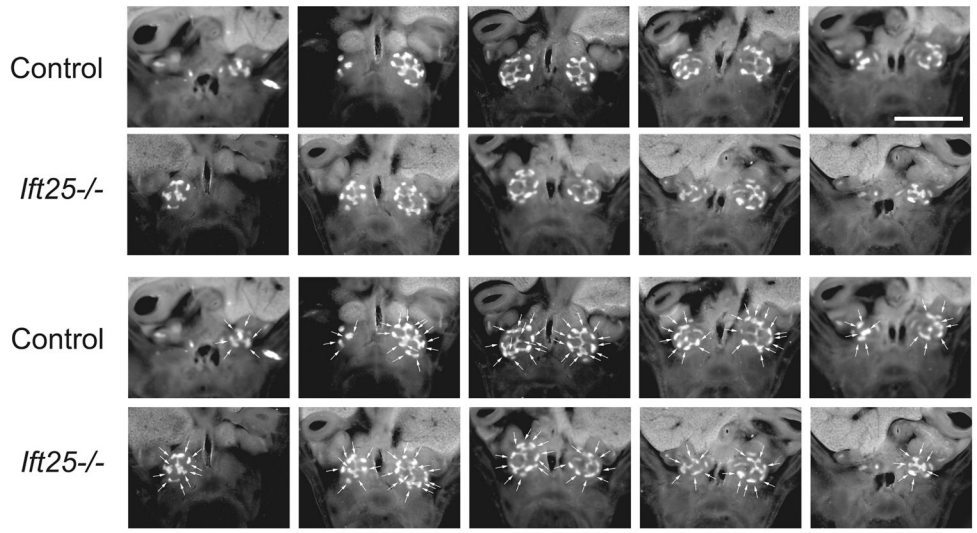

Figure 5. Reduced Numbers of Terminal End Buds On Ureteric Epithelium in *Ift25* Mutants

A. Images of serial sections of E13.5 control and *Ift25*$^{-/-}$ embryos with GFP-labeled (grey) ureteric epithelium. Scale bar is 1 millimeter.

B. Same as A except that arrows indicate terminal end buds. Control has 82.0±7.6 end buds, *Ift25*$^{-/-}$ has 62.7±6.5. Terminal end buds were marked with the genotype blinded. N=3 animals of each genotype. P=0.028 by unpaired t test.

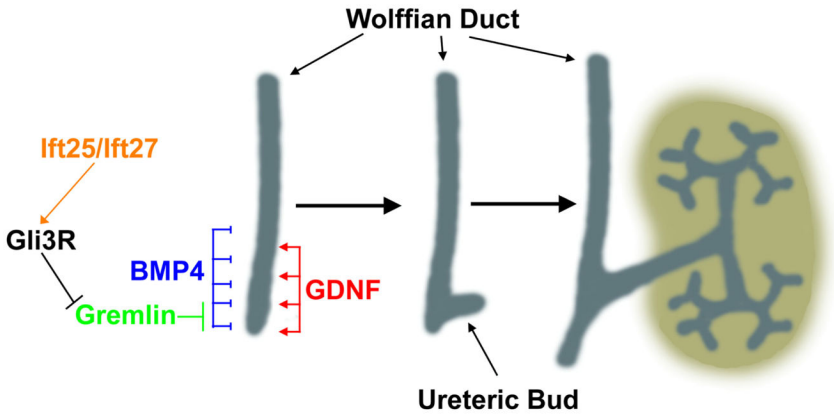

Figure 6. Model for the Role of Ift25 and Ift27 in Duplex Kidney Formation

GDNF produced by the metanephric mesenchyme promotes the formation of ureteric buds on the Wolffian duct. The activity of GDNF is antagonized by BMP4 to prevent bud formation. BMP4 is in turn antagonized by a small zone of gremlin to allow a single ureteric bud to form. In the developing limb, gremlin expression is antagonized by Gli3R. Loss of IFT25 or IFT27 reduces the amount of Gli3R produced. Thus, a possible mechanism for the duplex kidney in *Ift25* and *Ift27* mutants is that the reduced amount of Gli3R in these mutants allows the gremlin zone to expand allowing ectopic ureteric outgrowths to form leading to duplex kidneys. Model is modified from (Costantini and Shakya, 2006).